Faraday Discussions

RSC Publishing

Cite this: *Faraday Discuss.*, 2013, **164**, 19

PAPER

View Article Online
View Journal | View Issue

Microelectrochemical visualization of oxygen consumption of single living cells

Michaela Nebel,[a] Stefanie Grützke,[a] Nizam Diab,[b] Albert Schulte[c] and Wolfgang Schuhmann*[a]

Received 10th February 2013, Accepted 18th March 2013
DOI: 10.1039/c3fd00011g

The detection of cellular respiration activity is important for the assessment of the status of a biological cell. Due to its non-invasive character and high spatial resolution scanning electrochemical microscopy (SECM) is a powerful tool for single cell measurements. Common limitations of respiration studies performed by SECM are discussed and strategies provided to further adapt SECM detection schemes to the specific requirements for the investigation of single cell respiration. In particular the combination of a potential pulse technique in the redox competition mode of SECM with a shearforce-based constant-distance positioning of the SECM tip is proposed for characterising the impact of the tip reaction during SECM imaging. The adjustment of the driving force of the tip reaction and the selection of the time for data acquisition after applying the potential pulse allowed a successful visualization of cell respiration activity.

Introduction

Single cells, as the smallest independent unit of a living organism, facilitate the study of complex biochemical processes in a simplified manner. According to the principle of reductionism this simplification enables elucidating implications of the role of individual cells inside the whole organism, a better understanding of selected reaction pathways and the species involved therein.[1] A specific advantage of electrochemical methods in biological studies is that some of the most important species involved in biological processes like NO, catecholamine neurotransmitters, oxygen, and reactive nitrogen (RNS) or reactive oxygen species (ROS) are directly detectable under physiological and non-invasive conditions. Furthermore, microelectrodes facilitate local electrochemical investigations in the vicinity of an inspected cell and a first application was already described in

[a]*Lehrstuhl für Analytische Chemie – Elektroanalytik & Sensorik, Ruhr-Universität Bochum, Universitätsstr. 150, 44780 Bochum, Germany. E-mail: Wolfgang.Schuhmann@rub.de; Fax: (+49)234-32-14683; Tel: (+49) 2343226200*

[b]*Chemistry Department, Faculty of Arts and Sciences, The Arab American University, P.O. Box 240, Jenin, Palestine*

[c]*Biochemistry-Electrochemistry Research Unit, School of Chemistry and Biochemistry, Institute of Science, Suranaree University of Technology, Nakhon Ratchasima 30000, Thailand*

1976.[2] The flexibility of electrochemical detection schemes in combination with the broad range of traceable species led to an increasing number of different applications of stationary microelectrodes as reviewed *e.g.* in ref. 3. Scanning electrochemical microscopy (SECM)[4] as a spatially resolving microelectrochemical technique enables accurate positioning of a microelectrode accompanied by visualization of local electrochemical activity distributions. Beside the investigation of fluxes through the cellular membrane during exocytosis events[5,6] and the mapping of intracellular activity,[7–9] the detection of the respiration activity of individual cells is of high importance. The respiratory chain is directly connected with the metabolism of a cell and therefore the consumed oxygen is an essential measure of the cell status.

Due to a comparatively simple experimental setup and a fast detection procedure, a large number of single cell SECM investigations have been performed in the constant-height mode in which the SECM tip approaches the sample surface at *x*,*y*-coordinates far away from the specimen under investigation and scanned laterally keeping the *z*-position fixed.[10,11] In order to prove that the obtained constant-height SECM images were caused by the respiration activity of the cell, several studies utilized KCN to block mitochondrial respiration by inhibition of cytochrome c oxidase in complex IV of the respiratory chain.[10,12] A subsequent diminution or absence of a current decrease above the cell body is used as evidence for a successful visualization of cell respiration. These experiments are based on the assumption that the cell morphology is not changed due to respiration inhibition. However, it is known that morphology fluctuations occur during cell death, like *e.g.* swelling or shrinking. These variations are not considered but might influence the tip current.

Further refinements of the SECM detection scheme for single cell analysis were dedicated to strategies minimizing limitations of constant-height mode experiments. Beside the use of specially designed double barrel electrodes for the simultaneous detection of the tip-to-sample distance and the biological activity,[13,14] the embedding of cells into cavities,[15] the evaluation of SECM approach curves on top and at the side of the investigated cell,[16,17] and time-lapse SECM[18] have been reported. However, studies utilizing different redox mediators are based on the assumption that oxygen and the added mediator behave in a comparable way, *e.g.* showing similar diffusion coefficients. Furthermore, these strategies lack a true topography-free investigation of the structure–activity-relationships necessary for an in-depth understanding of cellular processes. Therefore, constant-distance mode (cd-mode) SECM experiments in which the tip follows the contour of the investigated cell in a continuously controlled and constant working distance are considered to be superior to constant-height mode investigations.

The easiest constant-distance mode is the constant-current mode in which the tip current is used for maintaining the working distance during the experiment and the stored *z*-position of the tip generates a visualization of the cell topography.[19,20] However, a basic requirement for a precise constant-current mode experiment is a uniform electrochemical activity of the investigated surface. Since the examination of variations in reaction rates at the sample surface is the intrinsic aim of SECM investigations, the constant-current mode is strongly limited in that respect. Alternatively, current-independent distance control mechanisms include the adjustment of the tip-to-sample distance by impedance-based signals,[21] through shearforce interactions,[22] and *via* merging other

scanning probe techniques like atomic force microscopy (AFM)[23] or scanning ion conductance microscopy (SICM).[24] Recently, these strategies have been successfully applied for cell investigations.[5,6,20,25–27]

An additional aspect often neglected in SECM respiration studies is the high permeability of the cell membrane for certain molecules and the consequent possibility of diffusional exchange across the lipid bilayer due to the formed concentration gradients. Therefore, we focus in this contribution on the elucidation of the complex interaction of different reaction rates involved in the SECM detection scheme for the investigation of the respiration activity of single living cells. Particularly, the influence of the driving force of the tip reaction on the overall result of the SECM experiment is investigated. In order to further study and control the role of the scanned tip, a potential pulse profile applied at the SECM tip in combination with a time dependent data acquisition is utilized.

Experimental

Cell cultures and solutions

Retzius cells were from medicinal leeches and cultured according to a procedure described in ref. 28. PC12 cells were grown on poly(ornithine)-covered glass slides as described in ref. 29, and transformed human umbilical vein endothelial cells (HUVEC cells) were cultured as reported previously.[13] Samples of PC12 and HUVEC were kindly provided by Dr A. Blöchl and Prof. Dr I. D. Dietzel-Meyer (Lehrstuhl für Molekulare Neurobiochemie, Ruhr-Universität Bochum, Germany). Human embryonic kidney cells (HEK293) were cultured as described in ref. 30 and were kindly supplied by Dr C. H. Wetzel (Lehrstuhl für Zellphysiologie, Ruhr-Universität Bochum, Germany). Measuring solutions contained 125 mM NaCl, 5 mM KCl, 1.2 mM NaH_2PO_4, 1 mM $CaCl_2$, 1.2 mM $MgCl_2$, 10 mM glucose and 25 mM 4-(2-hydroxyethyl)-1-piperazine-1-ethanesulfonic acid (HEPES), pH 7.4 for PC12 and for HUVEC. An extracellular solution with 140 mM NaCl, 5 mM KCl, 2 mM $CaCl_2$, 1 mM $MgCl_2$ and 10 mM HEPES, pH 7.3 were used for HEK293 cells. $K_4[Fe(CN)_6]$ for the determination of the tip-to-sample separation in the feedback mode was from Merck (Darmstadt, Germany) and used as received.

SECM experiments

SECM measurements have been performed with a Bio-SECM setup based on the instrument described in.[6] The positioning system of the SECM is mounted on an inverted microscope (Axiovert 25 C, Carl Zeiss, Jena, Germany with an integrated digital CCD camera from IDS Imaging Development Systems, Obersulm, Germany) allowing easy positioning of the tip next to the desired cells and continuous optical inspection of the cell status. The SECM positioning system consists of three orthogonal stepper motors (SPI Robot Systems, Oppenheim, Germany) with a nominal resolution of 10 nm per microstep and an additional piezo element (NanoCube P-611.ZS with an E-665 controller from Physik Instrumente, Waldbronn, Germany) for the *z*-direction. Furthermore, the SECM includes components necessary for the optical shearforce-based constant-distance mode with a laser (CDM 14S/S70/1, Atos, Pfungstadt, Germany), a split photodiode (Spot 4D, Laser2000, Wessling, Germany), a lock-in amplifier (model 5210, Ametek, Meerbusch, Germany), and an agitation piezo element (PSt 500/5/15,

Piezomechanik Pickelmann, München, Germany) for vibrating the tip in its characteristic resonance frequency. For constant-distance mode SECM experiments the laser is positioned at the end of the vibratory tip electrode. The resulting Fresnel diffraction pattern impinges on the split photodiode and the difference signal of the photodiode is used for the readout of the tip vibration. This signal is phase-sensitively amplified with respect to the sinus shaped agitation signal applied at the agitation piezo element *via* a lock-in amplifier and used for the current-independent distance control procedure. For electrochemical measurements a potentiostat model VA-10 (Npi Electronics, Tamm, Germany) was used together with an ADDA board (CIO-DAS 802/16, Plug-In Electronics, Eichenau, Germany) for potential control and data acquisition. All potentials were measured *versus* a miniaturized Ag/AgCl (3 M KCl) reference electrode in a two electrode configuration. The whole setup is controlled by software programmed in Visual Basic and placed on a vibration damped base inside a faraday cage.

SECM tips were vibratory 10 μm Pt electrodes fabricated according to ref. 31 for the PC12 cell experiments or otherwise highly flexible polymer-insulated and platinized carbon fibre electrodes with diameters of 7 to 9 μm fabricated following a procedure described in ref. 5, 6 & 32. Either a cathodic electrodeposition paint (ClearClad HSR401 from LVH coatings, UK) or alternatively an anodic paint (Canguard, BASF Coatings, Münster, Germany) were used for the insulation of the carbon fibres (type Grafil E/XA-S, Courtaulds Limited Carbon Fibres Division, Coventry, UK). The precipitation of the soluble polymer was repeated twice by means of a two-step procedure of subsequent precipitation invoked by an electrochemically induced pH shift and heat curing at 180 °C for 20 min in order to crosslink the precipitated polymer. After insulation and cutting to expose a fresh carbon surface, the carbon fibre electrodes were electrochemically characterised by means of cyclic voltammetry in a solution containing 5 mM $[Ru(NH_3)_6]Cl_3$ (ABCR, Karlsruhe, Germany) and 100 mM KCl (VWR International, Darmstadt, Germany). To enable oxygen detection, a thin layer of platinum was deposited on the fibre electrodes using a solution of 2 mM H_2PtCl_6 (Merck, Darmstadt, Germany) and potentiodynamic cycling (300 mV to −500 mV, scanrate: 100 mV s^{-1}, 3 cycles). The resonance frequency of the vibratory SECM tips was typically in the range of 0.5–5 kHz. A set point of 2–5% change from the shearforce signal in bulk was defined as the condition of the distance control procedure and used for the adjustment of the tip-to-sample separation. The corresponding magnitude value was kept constant during continuous shearforce-based constant-distance mode. For this purpose the *z*-position of the tip was adjusted after each lateral displacement *via* the *z*-piezo element until this set point was reached again. Alternatively, for 4D SF/CD-SECM[33] a magnitude change of 5% was defined as the stop criterion of the shearforce-based tip approach. At each grid point the tip was moved towards the sample surface under shearforce control until this change in the tip vibration was reached. After current detection at the point of closest approach, a retraction of the tip was accomplished in defined *z*-increments and the corresponding signal was measured at each of the different but constant tip-to-sample separations. Performing this sequence of shearforce-based positioning and subsequent retraction steps leads to a 4D dataset that includes complete current images in various constant working distances towards the topography contour of the sample surface.

Results and discussion

Limitations of constant-height mode SECM for single cell experiments

The most frequently used experimental approach for studying the respiration activity by means of SECM is a variation of the substrate-generation/tip-collection (SG/TC) mode. In this competitive SG/TC arrangement the tip is continuously polarized to the oxygen reduction potential in order to detect the amount of oxygen present in the gap between the tip and sample. Due to the competition between the tip and sample for the same amount of oxygen, a decrease of the reduction current of the scanned tip represents a locally higher respiratory activity of the investigated cell. An exemplary constant-height mode SECM experiment of adherently growing Retzius cells using this competition type SG/TC mode is displayed in Fig. 1.

The image shows clearly the expected current decrease above the pair of individual Retzius cells that correspond in size and shape with the optical appearance of the investigated cells. Although this image shows a clear contrast and good signal-to-noise ratio, the interpretation of this type of experiments might be more difficult than it initially seems to be. The delicate situation for the interpretation of oxygen measurements at living cells in constant-height mode SECM is explained in more detail in Fig. 2. A breathing cell decreases the oxygen concentration in its proximity and hence a smaller tip current is expected. However, the tip current is distance dependent. A decreased tip-to-sample distance leads likewise to a reduced tip current due to the hindered diffusion of oxygen from the bulk solution into the gap between the tip and sample. Due to the comparatively large dimensions of a cell body, which is comparable with the positioning distance of a conventional 10 μm diameter SECM tip, the topography contribution is not negligible. In order to demonstrate this superposition of both effects, a control experiment was performed, adding a freely diffusing redox mediator to determine the tip-to-sample separation (scheme in Fig. 2a) similar to an approach described by Gonsalves *et al.*[17] for array scan experiments. $[Fe(CN)_6]^{4-}$ was chosen as a hydrophilic mediator that does not cross the cell membrane and is therefore suitable to investigate the topography in the negative feedback mode.[7,8] The current signal of the competition arrangement in Fig. 2b shows a current decrease at the positions of the cells. Taking the tip current for the additionally added redox mediator into account (grey line in Fig. 2b) it

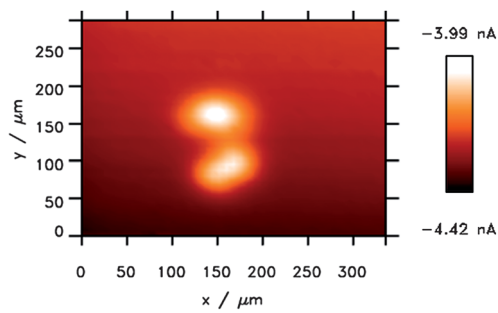

Fig. 1 Constant-height SG/TC mode SECM image of a pair of adherently growing Retzius cells from the medicinal leech in a competition mode arrangement.

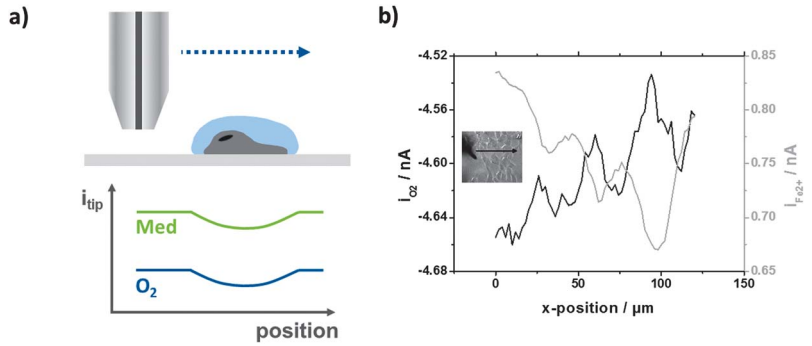

Fig. 2 (a) Scheme of the current signal in a constant-height mode SECM line scan across an adherently growing single cell. At each *x*,*y*-grid point the tip potential was changed between oxygen detection in a competition arrangement and the feedback mode detection of an additionally added free diffusing redox mediator for the investigation of the tip-to-sample distance. (b) SECM line scan across a HEK293 cell in a solution containing 0.5 mM $[Fe(CN)_6]^{4-}$. Tip: platinized carbon fibre electrode (diameter 7 µm), $E_{tip,O2} = -600$ mV, $E_{tip,Fe2+} = +500$ mV. (black line: O_2 reduction; grey line: $[Fe(CN)_6]^{4-}$ oxidation). Insert: Optical micrograph taken with the camera of the inverted microscope of the SECM setup showing the direction and position of the line scan.

becomes obvious that the topography expectedly affects the tip signal. Consequently, the particular challenge for respiration studies in constant-height mode at single cells is in fact seen; that a current decrease is caused on the one hand by the oxygen consumed by the living cell and on the other hand by a smaller tip-to-sample distance. As a matter of fact, a deconvolution of both contributions is difficult. This is even more important because oxygen consumption due to respiration is slow while the current decrease due to the negative feedback effect is substantial.

Beside this superposition of topographic and activity effects, the steep elevated structure of the cells leads to a high risk of contact between tip and cell body causing a mechanical stimulation or a destruction of the fragile cell membrane. Furthermore, the utilization of an additional redox mediator might influence the metabolism of the investigated cell. On the basis of these results it is obvious that a current-independent distance control mechanism is required for a reliable investigation of living cells.

Distance controlled SECM investigation in the competitive SG/TC mode

In order to overcome the above-mentioned drawbacks, shearforce-based constant-distance mode SECM experiments have been applied in a further step for SECM respiration studies. A line scan in the shearforce-based constant-distance mode utilizing the competitive SG/TC mode across a PC12 cell is shown in Fig. 3. The topographic line scan is represented by the *z*-position of the tip when the set point of the shearforce-based distance control is reached. The tip followed the contour of the PC12 cell in a working distance of about 100 to 200 nm, starting at a position above the Petri dish and moving in the direction of the PC12 cell body. The topography scan shows clearly the elevated structure of the cell body with a height of about 11 µm. Contrary to the expected current decrease, a current increase was detected above the cell body at the tip.

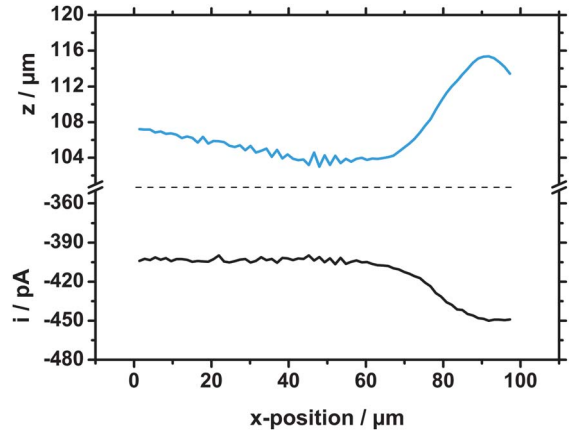

Fig. 3 Shearforce-based constant-distance mode SECM line scan above a PC12 cell. Investigation of the respiration activity in the competitive SG/TC mode beginning from a position above the Petri dish in the direction of the cell body.

Due to the semipermeability of the cell membrane, single cells exhibit similarities to a liquid/liquid interface in a SECM experiment.[34] At high oxygen reduction rates at the tip, a depletion of oxygen in the vicinity of the cell occurs. Oxygen is known to easily cross the cellular membrane.[8] As a result, a diffusional flux from the intracellular medium occurs along the concentration gradient, unintentionally leading to a situation similar to the previously described SECM-induced transfer (SECM-IT) mode.[35] Evidently, the living cell has to be considered like a sponge filled with oxygen and hence as an additional source for oxygen. The tip reaction actively intervenes and dominantly determines the oxygen concentration inside the gap between tip and cell which is even more pronounced due to the extremely short working distance established by shearforce positioning. As a matter of fact, this additional flux of oxygen interferes with the detection of respiration activity. Thus, the tip cannot be considered any longer as a passive spectator, which implies that the properties of the tip itself will largely alter the obtained SECM image. It is clear that under these conditions an error-free detection of cell respiration is impossible. Although this effect has been described in literature[8,17,26,27,36] it was not considered in cell respiration studies by means of SECM. Most studies try to circumvent this effect by using smaller electrodes; however, in order to achieve measurable currents even small electrodes may compete substantially with the slow impact of cell respiration on the oxygen concentration in the gap between tip and cell.

To verify this observation in more detail and to prove that the current increase is caused by the proposed transmembrane flux of oxygen into the gap, a control experiment was performed at another PC12 cell (Fig. 4). In contrast to the first experiment, $[Fe(CN)_6]^{4-}$ was added and used as redox mediator for an additional determination of the tip-to-sample distance in a negative feedback mode configuration. In a reliable constant-distance mode experiment no change in the oxidation current of $[Fe(CN)_6]^{4-}$ is expected.

In order to enable a simultaneous evaluation of two different redox species, the potential at the tip was changed at each point of the *x*,*y*-grid between −600 mV and

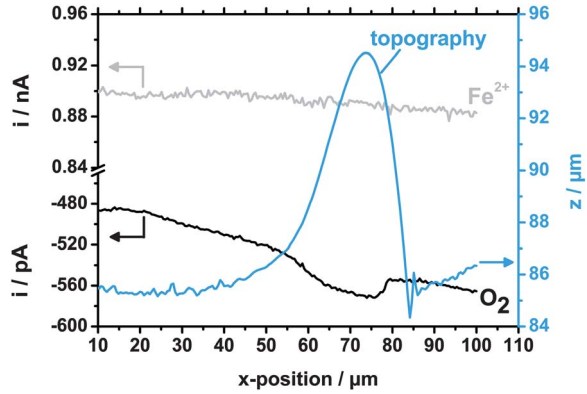

Fig. 4 Constant-distance mode SECM line scan above a PC12 cell in a cell buffer solution containing 30 µM $K_4[Fe(CN)_6]$ for the independent determination of the working distance in the feedback mode. The potential was changed between −600 mV for oxygen detection and +500 mV for the diffusion-limited oxidation of the $[Fe(CN)_6]^{4-}$ species. A current increase during oxygen detection was observed above the investigated cell. The oxidation current of $[Fe(CN)_6]^{4-}$ is not changed by passing the cell body, proving the accuracy of the shearforce distance control.

+500 mV, respectively. Again, the topography of the investigated cell body is clearly visualized using the shearforce-based *z*-positioning and a height of about 9 µm can be derived for the specific cell. As in the previous experiment an increase of the oxygen current was detected above the PC12 cell. However, no current change was observed for $[Fe(CN)_6]^{4-}$ oxidation proving the reliability of the shearforce-based constant-distance positioning. Hence, any possible impact of an error in the distance control can be excluded as the source for the unexpected increase in the oxygen reduction current above the cells. Furthermore, the observed behaviour is clearly due to the chosen experimental design and not an effect detected at a specific cell type that is demonstrated by Fig. 5 with the results of a 4D SF/CD-SECM experiment at a HEK293 cell. The detection procedure of the 4D SF/CD mode facilitates constant-distance mode experiments in various tip-to-sample separations. Therefore, this mode is able to visualize complete diffusion fields in front of a sample surface.[33] The topography image (Fig. 5a) clearly reflects the orientation and shape of the investigated cell agglomeration as shown in the optical micrograph (Fig. 5b). The tip current response is displayed in Fig. 5c. A current increase was detected above the investigated cells and confirms the results achieved with the PC12 cells.

In order to analyse further the distance dependence of the tip current, an electrochemical tomogram (Fig. 5d) was extracted from the 4D dataset at the line marked in Fig. 5c. The observed current increase reaches far into the solution and it is detectable even at a distance of 15 µm above the point of shearforce contact. Control experiments at glass beads and polymer spheres with comparable sizes to the cell bodies as model systems were performed to further evaluate the extraction of oxygen out of the cell body. As expected, no increase of the oxygen reduction current was observed during similar experiments to those shown in Fig. 5 using glass beads with a 10 µm diameter instead of the cells. However, if polystyrene beads of similar size were used to replace the cells, a small current increase was at least detected, most likely due to the soft outer layer of the beads which is soaked with electrolyte solution (results not shown).

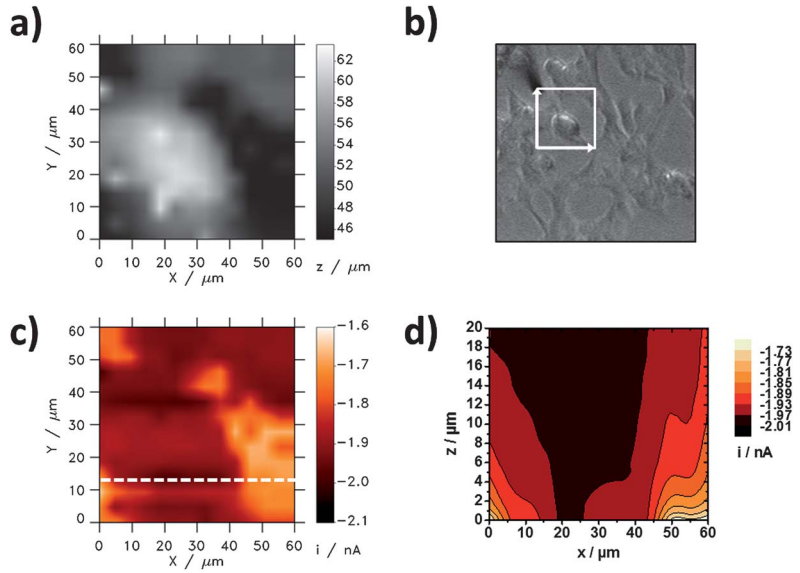

Fig. 5 Investigation of a HEK293 cell sample by means of 4D SF/CD-SECM in the competition mode arrangement. (a) Topography image displayed as the *z*-position of the tip after reacting the pre-set stop criterion (the point of closest approach) during the shearforce-based *z*-approach curve, (b) optical micrograph of the cell sample marking the investigated area and the scan directions. (c) Tip current in the plane of closest approach at $E_{tip} = -600$ mV. A significant current increase is observed above the inspected cell. (d) Electrochemical tomogram (*x*,*z*,*i*-image) extracted at the line marked in (c). The position of shearforce contact is defined as 0 µm.

Based on these observations three sources of oxygen can be supposed affecting the tip current: (1) Oxygen consumed by respiration activity of the investigated cell ($O_{2,R}$). The amount of oxygen consumed by a single cell during the timescale of a SECM experiment is supposed to be small compared to the overall oxygen dissolved in the measuring solution. The consumption of oxygen by a breathing cell causes only small current variations as compared with the high background current. (2) Oxygen that is transported from the bulk solution to the tip by diffusion ($O_{2,D}$). The diffusion of oxygen inside the gap depends on the working distance and on the geometrical size of the tip, thus a similar contribution is assumed for each tip-to-sample separation of the constant-distance mode experiment. (3) Oxygen reaching the tip due to permeation through the cell membrane ($O_{2,P}$). This flux is induced by a tip that consumes a large amount of oxygen in the surroundings of the inspected cell and evokes therefore a concentration gradient between the intracellular and extracellular medium. This contribution is not related to the cell activity and superimposes the current signal significantly.

Characterisation and adjustment of the influence of the tip reaction onto the overall imaging result

In order to visualize respiration activity successfully, a variation of the SECM detection scheme is required. The central parameter initiating a disturbance in the established detection procedure is the driving force of the oxygen reduction at

the tip electrode. A simple method to reduce the driving force is a decrease of the applied potential. However, even at a weak reduction potential of −200 mV visualization of cell respiration was not successful (data not shown). Further decreasing the electrode size or limiting the diffusion field in front of the tip through fast scan cyclic voltammetry (FSCV) or potential pulses are additional strategies to diminish the oxygen reduction rate. While FSCV enables the polarisation of the tip for short timescales and a detection of different redox species,[37] a time-resolved current detection during short timeframes is possible *via* the redox competition mode of scanning electrochemical microscopy (RC-SECM).[38] Originally designed for the investigation of heterogeneous oxygen reduction catalysts, the RC-SECM mode includes the competition between tip and catalyst sample for the oxygen inside the gap. Furthermore, oxygen depletion is avoided by a potential pulse profile applied at the tip comprising injection of oxygen by means of oxidative water splitting and a following oxygen competition pulse. During the competition pulse a time dependent current decay curve is recorded enabling a time-resolved analysis of the tip current response. Combining the detection scheme of the RC-SECM with the shearforce-based constant-distance mode leads to a SECM mode (SF/CD-RC-SECM, Fig. 6) that is able to limit the tip reaction by short potential pulses in a constant working distance.

The application of the SF/CD-RC-SECM to HUVEC cells is shown in Fig. 7. A crucial experimental detail is the choice of the potential applied during electrode movement. In order to minimize the overall amount of oxygen consumed by the tip, a potential of +500 mV was applied during the *z*-positioning and lateral motion of the tip to the next *x*,*y*-grid point. At this potential no oxygen reduction occurs in a buffer solution of pH 7.4. Immediately before the competition experiment, oxygen is injected by a short potential pulse to 1.4 V. The topography image of the investigated cell is shown in Fig. 7a and the corresponding optical micrograph of the cells with an indication of the scan area and scan direction is displayed in Fig. 7b. Due to the time-resolved data acquisition of the RC-SECM detection scheme, a dataset of 100 current images is achieved during one single array scan. A selection of current images at times of

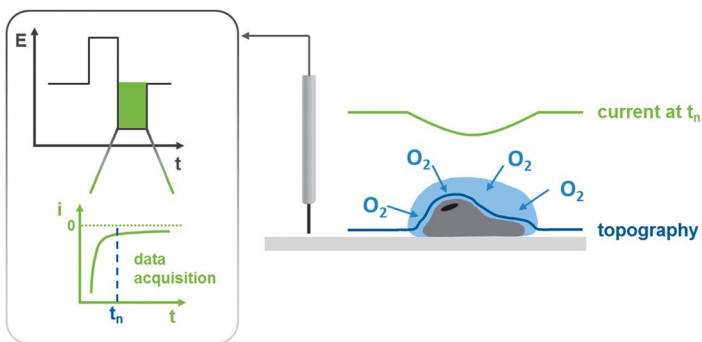

Fig. 6 Scheme of the redox competition mode (RC SECM) implemented in the shearforce-based constant-distance SECM. A flexible potential pulse profile is applied at the tip at each point of the *x*,*y*-grid. In a first pulse oxygen is injected in the gap through oxidative water splitting. During the following competition pulse, the tip and cell compete for the oxygen present inside the gap and a time-dependent data acquisition is realized leading to a transient detection scheme.

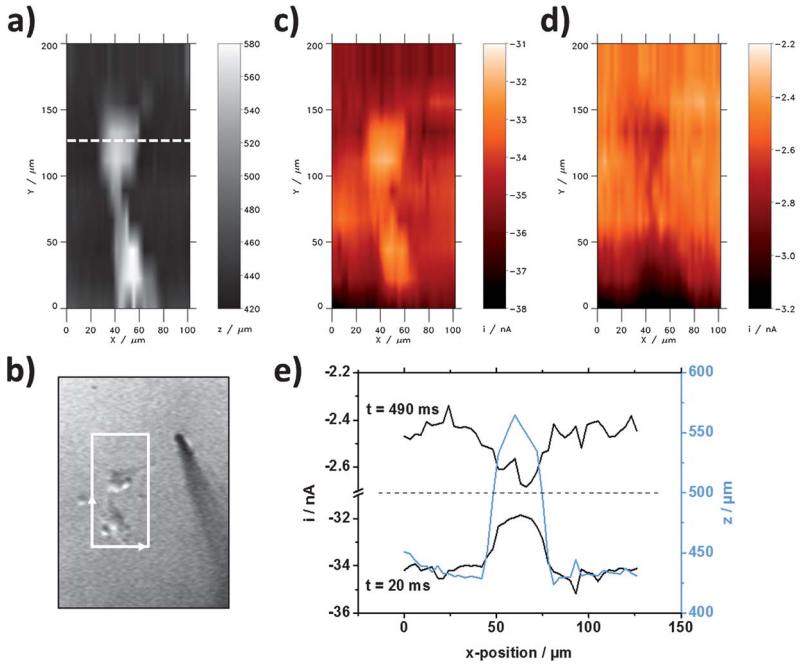

Fig. 7 Constant-distance mode SECM experiment in the RC mode at HUVEC cells. (a) Topography image of the investigated cells displayed as the tip *z*-position after establishing a constant working distance. (b) Optical micrograph of the investigated cells with a mark of the scanned area and the scan directions, (c) current signal at $t = 20$ ms and d) current image at $t = 490$ ms after the competition pulse was applied at the SECM tip. In both current images a lighter colour represents a current decrease while a current increase appears in a darker colour. (e) Line scans extracted from the array scans at the position marked in (a). Potential pulse profile: base potential: 0.5 V, pulse 1 (oxygen injection pulse): 0.2 s at 1.4 V, and pulse 2 (competition pulse): 0.5 s at −0.65 V.

20 ms and 490 ms after the competition pulse was applied are shown in Fig. 7c and figure 7d, respectively. For a direct comparison of both tip responses at the chosen acquisition times, line scans (Fig. 7e) have been extracted at the position marked in Fig. 7a.

At short pulse times a current decrease was observed directly above the inspected cell bodies. Obviously, the influence of the positioned tip was successfully diminished enabling a visualization of the locally reduced amount of oxygen due to cell respiration. However, during the course of the potential pulse a change of the tip signal was detected. At 490 ms after applying the competition pulse at the tip a current increase was measured at the *x*,*y*-positions where the topography image confirmed the presence of the cell body. At this time the expansion of the diffusion field in front of the tip electrode was sufficient to cause a depletion of oxygen inside the gap, thus disturbing the respiration detection. By means of the SF/CD-RC-SECM a visualization of the transition from a situation in which the tip acts as a passive observer to a tip that actively sucks out oxygen from the cell body was achieved. Furthermore, the time-dependent data acquisition of this detection scheme provides a tool to adapt the tip reaction to the unique requirements of the performed investigation of the cell activity.

Conclusions

The respiration activity of single cultured cells was investigated by means of constant-distance mode SECM and existing limitations of established detection procedures were presented. Furthermore, the influence of the reaction rate at the scanned tip was identified as the key element for a successful respiration study. In order to overcome restrictions arising from a high driving force of the electrochemical reaction at the SECM tip, a flexible potential pulse profile in combination with a time-dependent data acquisition was integrated in the detection scheme of the shearforce-based constant-distance mode. The proposed SF/CD-RC-SECM enabled a detailed study of the interaction of the involved reaction rates through the time-resolved detection procedure. At short pulse times a successful visualization of the respiration activity was achieved due to the minimized interference from the tip reaction. Additionally, the expanding diffusion field in front of the tip electrode within the duration of the applied competition pulse caused the formation of a concentration gradient that was compensated by a transmembrane diffusion of oxygen. At the end of the competition pulse the flux of oxygen from the intracellular medium to the outer side of the cell wall was superimposed over the contribution of the cell respiration. The SF/CD-RC-SECM detection scheme enabled the direct observation of the change from a passive observer that is able to detect the tiny changes in the local oxygen concentration caused by the breathing cell to an electrode that provokes actively a depletion of oxygen inside the gap between the tip and cell body and thus disturbing the respiration detection. Due to the detection of a series of individual current images at different pulse lengths during one single SF/CD-RC-SECM experiment, a detailed knowledge of the optimal time for the data acquisition is not required and the image with the best contrast can be chosen after the experiment was completed. For future work an additional reduction of the tip electrode size is proposed as a supplementary strategy to further decrease the amount of oxygen consumed by the scanned tip concomitantly increasing the lateral resolution.

Acknowledgements

The authors are thankful to all colleagues who contributed to this project over many years of attempts to finally detect oxygen consumption of living cells in a reliable way, particularly Dr Andreas Hengstenberg, Dr Sonnur Isik-Uppenkamp and Dr Kathrin Eckhard. Moreover, valuable discussions with Prof. Dr Tomokazu Matsue are acknowledged. Dr A. Blöchl and Prof. Dr I. D. Dietzel-Meyer (Lehrstuhl für Molekulare Neurobiochemie, Ruhr-Universität Bochum, Germany) as well as Dr D. Hollatz, S. Zielke and Dr C. H. Wetzel (Lehrstuhl für Zellphysiologie, Ruhr-Universität Bochum, Germany) are acknowledged for providing cell samples. This work was supported by the EU and the state NRW in the frame work of the HighTech.NRW program and the Center for Electrochemical Sciences – CES.

References

1 J. V. Sweedler and E. A. Arriaga, *Anal. Bioanal. Chem.*, 2006, **387**, 1–2.
2 R. N. Adams, *Anal. Chem.*, 1976, **48**, 1128A–1138A.
3 (*a*) C. Amatore, S. Arbault, M. Guille and F. Lemaitre, *Chem. Rev.*, 2008, **108**, 2585–2621; (*b*) A. Schulte and W. Schuhmann, *Angew. Chem., Int. Ed.*, 2007, **46**, 8760–8777; (*c*)

S. Borgmann, *Anal. Bioanal. Chem.*, 2009, **394**, 95–105; (*d*) A.-S. Cans and A. G. Ewing, *J. Solid State Electrochem.*, 2011, **15**, 1437–1450.
4 (*a*) A. J. Bard, F. R. F. Fan, J. Kwak and O. Lev, *Anal. Chem.*, 1989, **61**, 132–138; (*b*) R. C. Engstrom, M. Weber, D. J. Wunder, R. Burgess and S. Winquist, *Anal. Chem.*, 1986, **58**, 844–848.
5 A. Hengstenberg, A. Blöchl, I. D. Dietzel and W. Schuhmann, *Angew. Chem., Int. Ed.*, 2001, **40**, 905–908.
6 L. P. Bauermann, W. Schuhmann and A. Schulte, *Phys. Chem. Chem. Phys.*, 2004, **6**, 4003–4008.
7 B. Liu, S. Rotenberg and M. Mirkin, *Proc. Natl. Acad. Sci. U. S. A.*, 2000, **97**, 9855–9860.
8 B. Liu, W. Cheng, S. A. Rotenberg and M. V. Mirkin, *J. Electroanal. Chem.*, 2001, **500**, 590–597.
9 X. Li and A. J. Bard, *J. Electroanal. Chem.*, 2009, **628**, 35–42.
10 T. Yasukawa, Y. Kondo, I. Uchida and T. Matsue, *Chem. Lett.*, 1998, 767–768.
11 (*a*) T. Yasukawa, T. Kaya and T. Matsue, *Chem. Lett.*, 1999, 975–976; (*b*) M. Nishizawa, K. Takoh and T. Matsue, *Langmuir*, 2002, **18**, 3645–3649; (*c*) P. M. Diakowski and Z. F. Ding, *Phys. Chem. Chem. Phys.*, 2007, **9**, 5966–5974.
12 (*a*) T. Kaya, Y. S. Torisawa, D. Oyamatsu, M. Nishizawa and T. Matsue, *Biosens. Bioelectron.*, 2003, **18**, 1379–1383; (*b*) L. L. Zhu, N. Gao, X. L. Zhang and W. R. Jin, *Talanta*, 2008, **77**, 804–808.
13 S. Isik, M. Etienne, J. Oni, A. Blochl, S. Reiter and W. Schuhmann, *Anal. Chem.*, 2004, **76**, 6389–6394.
14 (*a*) S. Isik, J. Castillo, A. Blochl, E. Csoregi and W. Schuhmann, *Bioelectrochemistry*, 2007, **70**, 173–179; (*b*) T. Yasukawa, T. Kaya and T. Matsue, *Anal. Chem.*, 1999, **71**, 4637–4641.
15 (*a*) H. Shiku, T. Shiraishi, H. Ohya, T. Matsue, H. Abe, H. Hoshi and M. Kobayashi, *Anal. Chem.*, 2001, **73**, 3751–3758; (*b*) H. Shiku, T. Shiraishi, S. Aoyagi, Y. Utsumi, M. Matsudaira, H. Abe, H. Hoshi, S. Kasai, H. Ohya and T. Matsue, *Anal. Chim. Acta*, 2004, **522**, 51–58; (*c*) Y. S. Torisawa, T. Kaya, Y. Takii, D. Oyamatsu, M. Nishizawa and T. Matsue, *Anal. Chem.*, 2003, **75**, 2154–2158; (*d*) Y. Torisawa, H. Shiku, T. Yasukawa, M. Nishizawa and T. Matsue, *Sens. Actuators, B*, 2005, **108**, 654–659; (*e*) R. Obregon, Y. Horiguchi, T. Arai, S. Abe, Y. Zhou, R. Takahashi, A. Hisada, K. Ino, H. Shiku and T. Matsue, *Talanta*, 2012, **94**, 30–35.
16 M. Tsionsky, Z. G. Cardon, A. J. Bard and R. B. Jackson, *Plant Physiol.*, 1997, **113**, 895–901.
17 M. Gonsalves, A. L. Barker, J. V. Macpherson, P. R. Unwin, D. O'Hare and C. P. Winlove, *Biophys. J.*, 2000, **78**, 1578–1588.
18 (*a*) Y. Hirano, Y. Nishimiya, K. Kowata, F. Mizutani, S. Tsuda and Y. Komatsu, *Anal. Chem.*, 2008, **80**, 9349–9354; (*b*) M. M. N. Zhang, Y.-T. Long and Z. Ding, *J. Inorg. Biochem.*, 2012, **108**, 115–122.
19 (*a*) J. M. Liebetrau, H. M. Miller, J. E. Baur, S. A. Takacs, V. Anupunpisit, P. A. Garris and D. O. Wipf, *Anal. Chem.*, 2003, **75**, 563–571; (*b*) W. Wang, Y. Xiong, F.-Y. Du, W.-H. Huang, W.-Z. Wu, Z.-L. Wang, J.-K. Cheng and Y.-F. Yang, *Analyst*, 2007, **132**, 515–518; (*c*) P. Sun, F. O. Laforge, T. P. Abeyweera, S. A. Rotenberg, J. Carpino and M. V. Mirkin, *Proc. Natl. Acad. Sci. U. S. A.*, 2008, **105**, 443–448; (*d*) Y. Takahashi, A. I. Shevchuk, P. Novak, B. Babakinejad, J. Macpherson, P. R. Unwin, H. Shiku, J. Gorelik, D. Klenerman, Y. E. Korchev and T. Matsue, *Proc. Natl. Acad. Sci. U. S. A.*, 2012, **109**, 11540–11545.
20 R. T. Kurulugama, D. O. Wipf, S. A. Takacs, S. Pongmayteegul, P. A. Garris and J. E. Baur, *Anal. Chem.*, 2005, **77**, 1111–1117.
21 M. A. Alpuche-Aviles and D. O. Wipf, *Anal. Chem.*, 2001, **73**, 4873–4881.
22 (*a*) M. Ludwig, C. Kranz, W. Schuhmann and H. E. Gaub, *Rev. Sci. Instrum.*, 1995, **66**, 2857–2860; (*b*) P. I. James, L. F. Garfias-Mesias, P. J. Moyer and W. H. Smyrl, *J. Electrochem. Soc.*, 1998, **145**, L64–L66; (*c*) B. Ballesteros Katemann, A. Schulte and W. Schuhmann, *Chem.–Eur. J.*, 2003, **9**, 2025–2033.
23 J. V. Macpherson, P. R. Unwin, A. C. Hillier and A. J. Bard, *J. Am. Chem. Soc.*, 1996, **118**, 6445–6452.
24 D. J. Comstock, J. W. Elam, M. J. Pellin and M. C. Hersam, *Anal. Chem.*, 2010, **82**, 1270–1276.
25 (*a*) X. C. Zhao, P. M. Diakowski and Z. F. Ding, *Anal. Chem.*, 2010, **82**, 8371–8373; (*b*) S. Isik and W. Schuhmann, *Angew. Chem., Int. Ed.*, 2006, **45**, 7451–7454; (*c*) R. J. Fasching, S. J. Bai, T. Fabian and F. B. Prinz, *Microelectron. Eng.*, 2006, **83**, 1638–1641.
26 Y. Takahashi, Y. Hirano, T. Yasukawa, H. Shiku, H. Yamada and T. Matsue, *Langmuir*, 2006, **22**, 10299–10306.
27 Y. Takahashi, A. I. Shevchuk, P. Novak, Y. Murakami, H. Shiku, Y. E. Korchev and T. Matsue, *J. Am. Chem. Soc.*, 2010, **132**, 10118–10126.
28 I. D. Dietzel, P. Drapeau and J. G. Nicholls, *J. Physiol.*, 1986, **372**, 191–205.
29 L. A. Greene and A. S. Tischler, *Proc. Natl. Acad. Sci. U. S. A.*, 1976, **73**, 2424–2428.

30 K. Klasen, D. Hollatz, S. Zielke, G. Gisselmann, H. Hatt and C. H. Wetzel, *Pfluegers Arch.*, 2012, **463**, 779–797.
31 A. Hengstenberg, C. Kranz and W. Schuhmann, *Chem.–Eur. J.*, 2000, **6**, 1547–1554.
32 A. Schulte and R. H. Chow, *Anal. Chem.*, 1996, **68**, 3054–3058.
33 M. Nebel, K. Eckhard, T. Erichsen, A. Schulte and W. Schuhmann, *Anal. Chem.*, 2010, **82**, 7842–7848.
34 S. Amemiya, J. D. Guo, H. Xiong and D. A. Gross, *Anal. Bioanal. Chem.*, 2006, **386**, 458–471.
35 A. L. Barker, J. V. Macpherson, C. J. Slevin and P. R. Unwin, *J. Phys. Chem. B*, 1998, **102**, 1586–1598.
36 K. Nagamine, Y. Takahashi, K. Ino, H. Shiku and T. Matsue, *Electroanalysis*, 2011, **23**, 1168–1174.
37 (*a*) L. Díaz-Ballote, M. Alpuche-Aviles and D. O. Wipf, *J. Electroanal. Chem.*, 2007, **604**, 17–25; (*b*) D. S. Schrock, D. O. Wipf and J. E. Baur, *Anal. Chem.*, 2007, **79**, 4931–4941; (*c*) D. S. Schrock and J. E. Baur, *Anal. Chem.*, 2007, **79**, 7053–7061; (*d*) K. L. Adams, M. Puchades and A. G. Ewing, *Annu. Rev. Anal. Chem.*, 2008, **1**, 329–355.
38 (*a*) K. Eckhard, X. Chen, F. Turcu and W. Schuhmann, *Phys. Chem. Chem. Phys.*, 2006, **8**, 5359–5365; (*b*) K. Eckhard and W. Schuhmann, *Electrochim. Acta*, 2007, **53**, 1164–1169.

